Official journal of the American Society of Gene & Cell Therapy

MTOpen

Inhibiting Notch Activity in Breast Cancer Stem Cells by Glucose Functionalized Nanoparticles Carrying γ-secretase Inhibitors

Veronika Mamaeva[1–3], Rasmus Niemi[1,2], Michaela Beck[4], Ezgi Özliseli[1,5], Diti Desai[5], Sebastian Landor[1,2,6], Tove Gronroos[7,8], Pauliina Kronqvist[9], Ina KN Pettersen[10], Emmet McCormack[3,11], Jessica M Rosenholm[5], Mika Linden[4] and Cecilia Sahlgren[1,2,12]

[1]Turku Centre for Biotechnology, University of Turku and Åbo Akademi University, Turku, Finland; [2]Faculty of Science and Engineering, Åbo Akademi University, Turku, Finland; [3]Department of Clinical Science, University of Bergen, Bergen, Norway; [4]Inorganic Chemistry II, Ulm University, Ulm, Germany; [5]Pharmaceutical Sciences Laboratory, Faculty of Science and Engineering, Åbo Akademi University, Turku, Finland; [6]Department of Cell and Molecular Biology, Karolinska Institutet, Stockholm, Sweden; [7]Turku PET Centre, University of Turku, Turku, Finland; [8]Medicity Research Laboratories, University of Turku, Turku, Finland; [9]Department of Pathology, University of Turku, Turku, Finland; [10]Department of Biomedicine, University of Bergen, Bergen, Norway; [11]Department of Medicine, Haematology Section, Haukeland University Hospital, Bergen, Norway; [12]Department of Biomedical Engineering, Technical University of Eindhoven, Institute for Complex Molecular Systems, Eindhoven, the Netherlands

Cancer stem cells (CSCs) are a challenge in cancer treatment due to their therapy resistance. We demonstrated that enhanced Notch signaling in breast cancer promotes self-renewal of CSCs that display high glycolytic activity and aggressive hormone-independent tumor growth *in vivo*. We took advantage of the glycolytic phenotype and the dependence on Notch activity of the CSCs and designed nanoparticles to target the CSCs. Mesoporous silica nanoparticles were functionalized with glucose moieties and loaded with a γ-secretase inhibitor, a potent interceptor of Notch signaling. Cancer cells and CSCs *in vitro* and *in vivo* efficiently internalized these particles, and particle uptake correlated with the glycolytic profile of the cells. Nanoparticle treatment of breast cancer transplants on chick embryo chorioallantoic membranes efficiently reduced the cancer stem cell population of the tumor. Our data reveal that specific CSC characteristics can be utilized in nanoparticle design to improve CSC-targeted drug delivery and therapy.

Received 16 December 2015; accepted 12 February 2016; advance online publication 29 March 2016. doi:10.1038/mt.2016.42

INTRODUCTION

Cancer stem cells (CSC) or "tumor-initiating cells" have been identified in various cancers including breast, colon, hematopoietic, and brain cancer.[1–5] The CSC population is not only important for tumor initiation, but it is also linked to metastasis, therapy resistance, and recurrence.[6] Approaches to target the CSC population can enhance the success of conventional therapies and change the outcomes of treatments. Detailed understanding of the biology of cancer stem cell survival and resistance, and the discovery of specific characteristics of CSCs will open up new possibilities for therapeutic intervention.[7–9]

Signaling pathways that are critical for stem cell function during development, such as the Wnt, Hedgehog, and Notch pathways are often deregulated in cancers, and promote survival and self-renewal of CSCs. Of these pathways, oncogenic Notch mutations occur in lymphoblastic leukemias, as well as in a variety of solid tumors including breast and non-small-cell lung cancer, colon, and prostate.[10,11] In breast cancer cells, Notch is linked to aggressive metastatic growth and therapy resistance.[12–17] Notch signaling has been implicated to regulate the CSC population in several forms of cancer, where it has been shown to be critical for maintenance and self-renewal of CSCs.[18–22] Notch-targeted therapy is thus an interesting treatment option and several clinical trials have been launched to test efficacy and safety of Notch inhibitors in cancer.[13,23,24] Despite the availability of efficient Notch inhibitors such as γ-secretase inhibitors (GSIs), peptides, antibodies or probodies, Notch-related treatments are currently prevented by side effects, due to the requirement for Notch signaling in most tissues.[19,24] GSI treatment induces diarrhea and suppression of lymphopoiesis.[25,26] Antibody-based targeting of Notch ligands is associated with induction of vascular tumors in mice[27] and a variety of side effects including headache, hypertension, fatigue, right, and left ventricular dysfunction in patients in clinical trials.[28] Therefore, clinically efficient suppression of Notch activity requires more targeted delivery strategies, and efficient delivery to CSCs to target Notch signaling in this population.

Nanotechnology has been promoted as *the* technology for targeted drug delivery to overcome problems with poor bioavailability, efficacy, and adverse side effects, and has recently been proposed as a candidate for CSC-targeted cancer therapeutics.[29–31] Data gained over the last decade demonstrate successful therapeutic action of various nanocarriers both *in vivo* in preclinical models and in clinical tests.[32–35] Among nanomaterials, we and others have recently demonstrated mesoporous silica particles (MSNs) to be highly versatile and efficient drug carriers in both conventional and novel cancer therapies.[36,37] MSNs can carry a high payload of hydrophobic drugs, such as GSIs.[38–41] We have previously shown successful breast tumor targeting of MSNs, and demonstrated that

R.N. and M.B. contributed equally to this work.

Correspondence: *Cecilia Sahlgren, Turku Centre for Biotechnology, University of Turku and Åbo Akademi University, FI-20520 Turku, Finland. E-mail: cecilia.sahlgren@btk.fi; c.m.sahlgren@tue.nl*

the carrier is suitable for intravenous, local and oral administration, and that it localizes to tumor tissue, and is biodegradable and eliminated through renal excretion.[38] In further support for the technology, MSNs in the form of C-dots (Cornell dots) have been approved by US FDA for stage I clinical trial.[42] Specific functionalization of the nanoparticles to enhance targetability to specific cell populations can expand the use of MSNs to efficient delivery of drugs to CSCs.

Here we identify specific phenotypic features of breast CSCs and utilize these features to design nanoparticles for efficient delivery and therapeutic efficacy of stem cell inhibitors. We demonstrate that Notch signaling is required for self-renewal of breast CSCs and for estrogen independent growth *in vitro* and *in vivo*, where it provides resistance toward estrogen-targeted therapies. We further show that Notch drives glycolytic metabolism and induces glycolytic switch in cancer cells. Intriguingly, we demonstrate that the breast CSCs display enhanced glucose uptake as compared to normal breast cancer cells. Utilizing these CSC features, we functionalized MSNs, carrying Notch inhibitors, with glucose analogues to efficiently deliver Notch signaling inhibitors to CSCs. Our data show that the functionalized particles target and are internalized by CSCs, and that the particles reduce the CSC pool and suppress tumor growth *in vitro* and *in vivo* in the chick embryo chorioallantoic- and murine xenograft-models.

RESULTS

Notch signaling induces cancer stem cells and enhances tumor growth

Notch signaling is activated by ligands on neighboring cells, inducing proteolytic processing of the receptor and releasing the intracellular domain (Notch intracellular domain) of the receptor, which translocates to the nucleus where it induces expression of downstream genes.[11] To explore the influence of Notch signaling activity on breast tumor growth and on the cancer stem cell population, we used our previously engineered MCF7 breast cancer cells which express high, basal (normal), and reduced Notch activity by stable expression of constructs NICD1-GFP, GFP, and dominant-negative CSL-GFP.[22] CSL is a key component of the Notch transcriptional complex. The cells are referred to as ^{high}Notch, ^{normal}Notch, and ^{low}Notch cells, respectively.[22] In line with our previous data,[22] tumors initially developed from all three cell lines upon orthotopical xenotransplantation. At 9 weeks, the ^{high}Notch cell-derived tumors showed dramatically enhanced tumor size coupled to increased proliferation compared with ^{normal}Notch cell as shown by expression of Ki67 (**Figure 1a**,**b**). The ^{high}Notch tumors exhibited increased expression of CD44, a widely used marker for CSCs (**Figure 1a**). CSCs can self-renew and sustain clonal growth. To test the capacity for self-renewal of ^{high}Notch, ^{normal}Notch, and ^{low}Notch cells, we plated a very low number of cells from each group on low adherence plates in serum free medium supplemented with growth factors and followed formation of spheroids. Spheroids were subsequently collected, dissociated, and replated. ^{high}Notch cells formed considerably higher numbers of, and bigger spheroids than ^{normal}Notch, and could sustain several cycles of dissociation and replating, whereas the ^{low}Notch cells were unable to form spheroids (**Figure 1c**). To further verify the CSC phenotype, we xenotransplanted 1,000 ^{high}Notch, ^{normal}Notch, and ^{low}Notch cells in mice, as only CSCs have the capacity to initiate tumor growth when a very low number of cells is implanted. Tumors were observed in 3 of 5 mice transplanted with ^{high}Notch, whereas ^{normal}Notch, and ^{low}Notch cells did not form tumors within 3 months after transplantation. Histological analyses characterized the tumors as aggressive invasive carcinoma (**Figure 1d**).

Induced Notch activity reduces the amount of estrogen receptors *in vitro* and *in vivo* and maintains cell growth in the absence of estrogens

Notch has been implicated in resistance to therapy targeting hormone receptor signaling in breast cancer. MCF7 cells express the estrogen receptor (ER) and are dependent on estrogen for growth *in vitro* and *in vivo*. When ^{high}Notch and ^{normal}Notch MCF7 cells were grown in hormone depleted medium, 25% of ^{normal}Notch cells died within 24 hours whereas the number of dead ^{high}Notch cells was considerably lower, around 10% (**Figure 2a**). When tumors were immunolabeled for ER, ^{high}Notch tumors displayed reduced amounts of receptors as compared to ^{normal}Notch tumors (**Figure 2b**). To test if estrogen independence was associated with the cancer stem cell population, we tested the ability of the ^{high}Notch CSCs to grow *in vivo* in the absence of estrogen supplements. Mice were gonadectomized to prevent physiological production of estrogen. We transplanted 25000 cells from dissociated spheroids in control and gonadectomized mice without estrogen supplement. α6 integrin expression in the spheroids confirmed the stem cell phenotype (**Figure 2c**). Tumors developed in four out of six mice transplanted with ^{high}Notch CSCs. Initial tumor growth in gonadectomized mice without estrogen supplement was slower, than in the control group but at 7 weeks the tumors in the two groups were comparable in size (**Figure 2d**). Immunohistochemistry analyses of the tumors verified the cancer stem cell phenotype by the high expression of CD44 (**Figure 2e**). The tumors also expressed high levels of the cytokeratins 5/6, which are indicators of a basal like cancer phenotype, as well as the proliferation marker Ki67. Further, the tumors showed no expression of ERs (**Figure 2e**). This data indicate that the ^{high}Notch CSCs are estrogen-independent and that Notch might promote resistance to estrogen targeted therapy in CSCs, in line with previous suggestions.[26]

Glucose uptake is enhanced in cancer stem cells and cancer cells with elevated Notch activity

We have previously shown that Notch signaling promotes a glycolytic phenotype and enhances glucose uptake in breast cancer.[22] To know if tumors with high Notch activity and enriched with CSCs also display enhanced glucose uptake *in vivo* we analyzed ^{high}Notch and ^{normal}Notch tumors with ^{18}F-fluorodeoxyglucose Positron Emission Tomography (^{18}F-FDG PET). ^{18}F-FDG PET revealed that tumors from ^{high}Notch cells showed increased glucose uptake, compared to control tumors (**Figure 3a**), in line with our previous results.[22] CSCs have been proposed to display a different metabolic phenotype than cancer cells. To assess glucose uptake in CSCs versus cancer cells we analyzed glucose uptake in adherent MCF7 and MDA-MB-231 breast cancer cells (adherent plate) and in CSC spheroids (spheroid plate) of the same cell lines using fluorescently labeled deoxyglucose (2NBDG). Cells

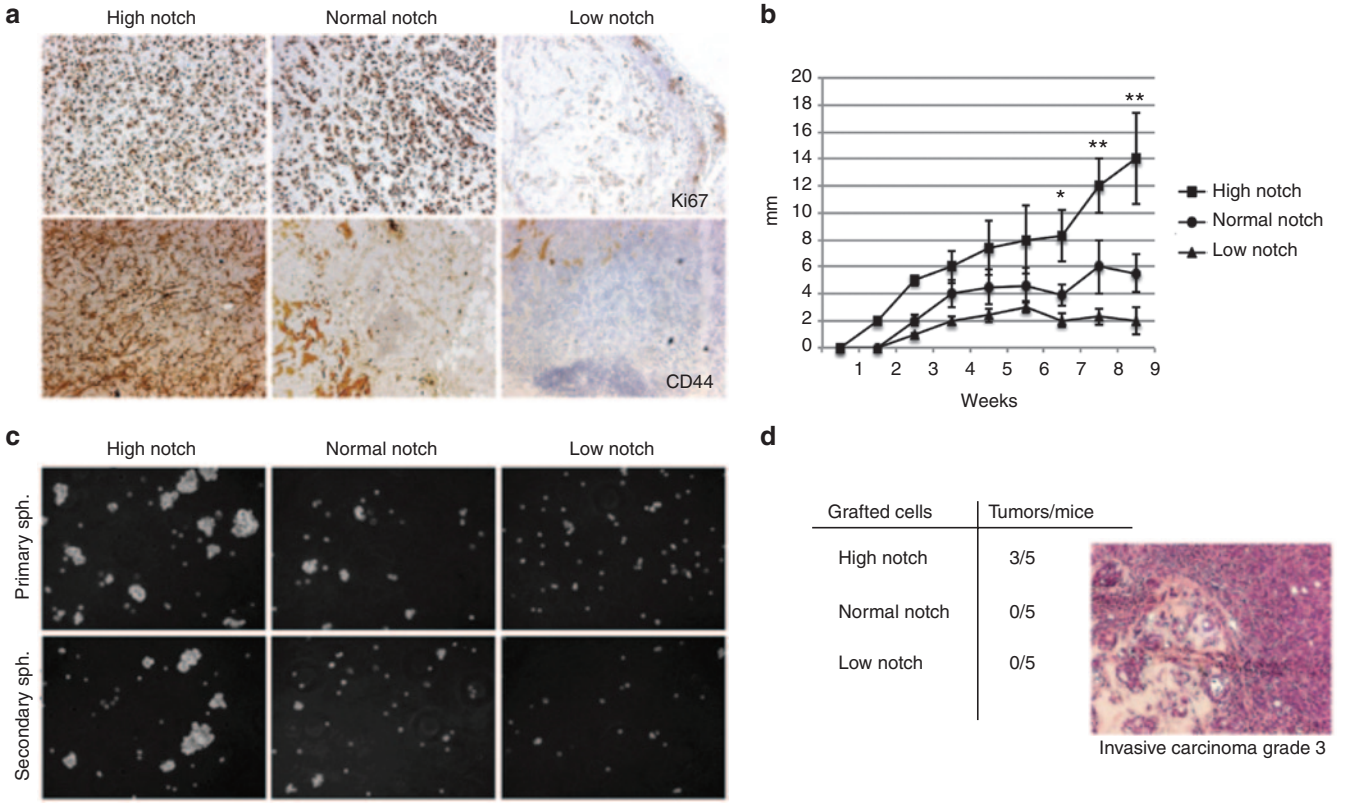

Figure 1 Notch activation enhances tumor growth. (**a**) Expression of the proliferation marker Ki67 and the stem cell marker CD44 in ^{high}Notch, ^{medium}Notch, and ^{low}Notch tumors at 9 weeks. ^{low}Notch shows mainly connective tissue. (**b**) Tumor diameter after xenografting in nude mice ($n = 6$ per group). (**c**) Primary and secondary spheroid formation by ^{high}Notch, ^{medium}Notch, and ^{low}Notch. Light microscopy images were obtained with 20× magnification (**d**) Number of tumors formed/mice xenotransplanted with 1,000 ^{high}Notch, ^{medium}Notch, and ^{low}Notch cells. Histology of ^{high}Notch tumors resembles that of human grade 3 invasive carcinoma. Statistical significance is denoted by $^{*}P \leq 0.05$, $^{**}P \leq 0.01$.

enriched for CSCs (spheroid plate) showed enhanced glucose uptake at both time points (**Figure 3b,c**). The difference in glucose uptake between cancer cells and CSCs was more pronounced in MCF7 cells, which can be explained by the fact that MCF7 cells per se are less glycolytic than MDA-MB-231 cells, whereas the CSC population in both cell lines is highly glycolytic. The difference in glycolytic profiles between MDA-MB-231 and ^{low}Notch MCF7 cells was further confirmed by measuring the lactic acid production, *i.e.*, extracellular acidification rate (ECAR) with Seahorse analyzer (Seahorse Bioscience) (**Supplementary Figure S1**). The difference in ECAR between the glucose-stimulated and oligomycin-treated conditions represents the spare glycolytic capacity, or glycolytic reserve, which was lower in ^{low}Notch MCF7 than in MDA-MB-231 cells (**Supplementary Figure S1**). Cells with a low spare glycolytic capacity are likely to be more dependent on glycolysis, whereas cells with a higher glycolytic reserve capacity should be more tolerant of metabolic stress. The data is in line with our previous data where we show that blocking of Notch induces glucose addiction.[22]

Synthesis of glucose-decorated mesoporous silica nanoparticles for γ-secretase delivery

Our data show that Notch activation enhances glucose uptake and promotes aggressive hormone-independent tumor growth *in vivo*. As Notch signaling is critical for self-renewal of the CSCs, and as CSCs display a metabolic phenotype characterized by enhanced glucose uptake, we decided to utilize the metabolic phenotype to target the CSCs with Notch inhibitors. We aimed to enhance particle uptake in CSCs by utilizing the machinery for cellular import of glucose and using glucose derivatives (glucose and glucosamine and glucuronic acid) as affinity ligands on the MSNs. A schematic representation of the strategy is shown in **Figure 4**. MSNs were chosen due to their characteristic ability to carry, especially poorly water soluble, payload within their molecular-sized pores; and for their flexible surface functionalization possibilities.[19–21] MSNs also have a previously proven ability for efficient delivery of GSIs, and for improved therapeutic efficacy in breast cancer.[38] Further, our previous work has demonstrated that sugar decorated MSNs efficiently deliver apoptotic drugs to cancer cells *in vitro*.[43] In that work, a hyperbranched surface polymer polyethlyleminine (PEI) was used as linker between the MSNs and the glucose entity and compared to MSNs where the glucose was attached directly to the amino-functionalized particle surface without linker. Two different conjugation mechanisms were chosen to attach the glucose moiety to the hyperbranched PEI layer: direct attachment of glucose to the terminal amino groups via activation of free hydroxyl groups on the glucose molecule (MSN-PEI-Gluc) and activation of the –COOH groups of glucuronic acid with subsequent amine conjugation under aqueous (MSN-PEI-GA_{aq}) or organic (MSN-PEI-GA_{org}) conditions. Here, we chose the same strategy for CSC

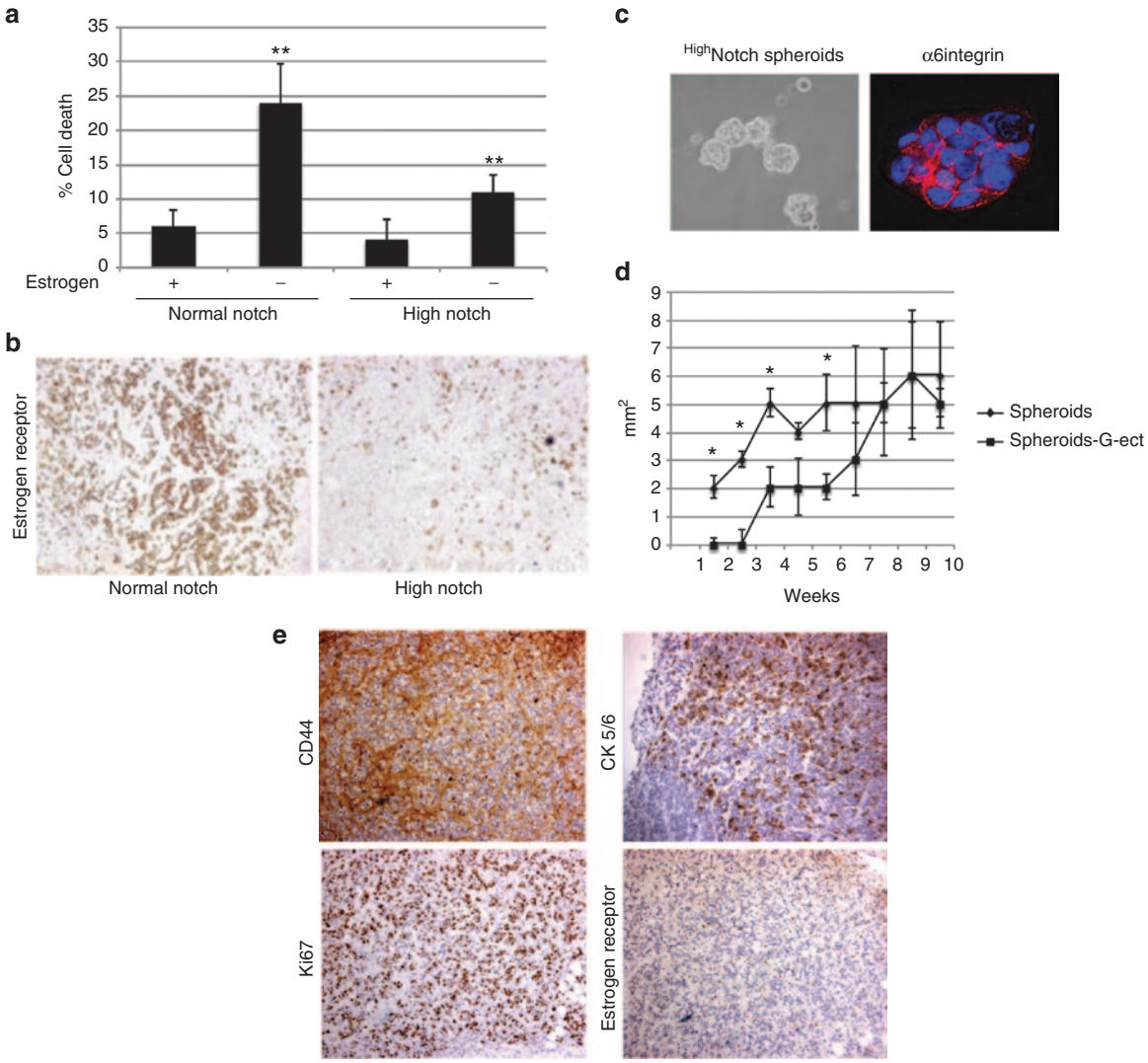

Figure 2 Notch signaling promotes estrogen-independent growth. (**a**) FACS analyses of propidium iodide-labeled ^{high}Notch, ^{medium}Notch cells grown in the presence or absence of estrogen. (**b**) Expression of the estrogen receptor in ^{high}Notch and ^{medium}Notch tumors. (**c**) ^{high}Notch cancer stem cells (CSCs) spheroids expressing the stem cell marker α6integrin were dissociated and 25,000 speroidal CSCs were orthotopically transplanted in gonadectomized mice. (**d**) Graph shows average growth of tumors in five animals derived from spheroids in control (Spheroids) and gonadectomized (Spheroids G-ect) mice (**e**) Immunohistochemistry of Spheroids G-ect tumors showing the expression of CD44, cytokeratin 5/6, Ki67 and the estrogen receptor. Statistical significance is denoted by $^{*}P \leq 0.05$, $^{**}P \leq 0.01$.

targeting, and continued to evaluate the particles for GSI delivery and therapeutic efficacy *in vitro* and *in vivo*. In addition, we chose an alternative strategy and linked glucosamine directly to carboxyl-functionalized particles via amide bond formation under mild conditions, after the carboxyl groups on the particles had been activated by conversion into NHS-esters. On all particles, the glucose moieties were accessible to interact with the glucose import systems of the cells. For characterization of the nanoparticles see **Supplementary Figures S2–S5**. All particles were highly monodisperse. The particles where the glucose entity was directly linked to the particle surface had a diameter of 180 nm, whereas the particles to which the glucose moiety was linked via the polymer structure had a diameter of 250–300 nm. The particles were functionalized either with fluorescein isothiocyanate for *in vitro* studies or with the fluorescent probe Atto647, the latter of which is more suitable for *in vivo* imaging.

Glucose functionalized particles are internalized by cancer cells and cancer stem cells *in vitro* and *in vivo*

Next we evaluated the uptake of glucose-decorated particles in breast cancer cells by flow cytometry (FACS) analyses. MDA-MB-231 breast cancer cell were incubated with particles for 4 hours prior to FACS analyses. Direct attachment of glucose to PEI functionalized particles under organic (MSN-PEI-GA_{org}) conditions demonstrated the highest uptake among the particles with the hyperbranched PEI layer (**Supplementary Figure S6a**), and this particle was chosen for subsequent experiments. Hence, the subsequent analyses were performed using the following particles: particles with direct conjugation of glucose: MSN-G (control particles MSN); and particles with conjugation of glucose via a PEI linker: MSN-PEI-GA_{org} (control particles MSN-PEI). The corresponding particles without glucose-functionality were used as controls. Both sets of particles demonstrated a higher uptake

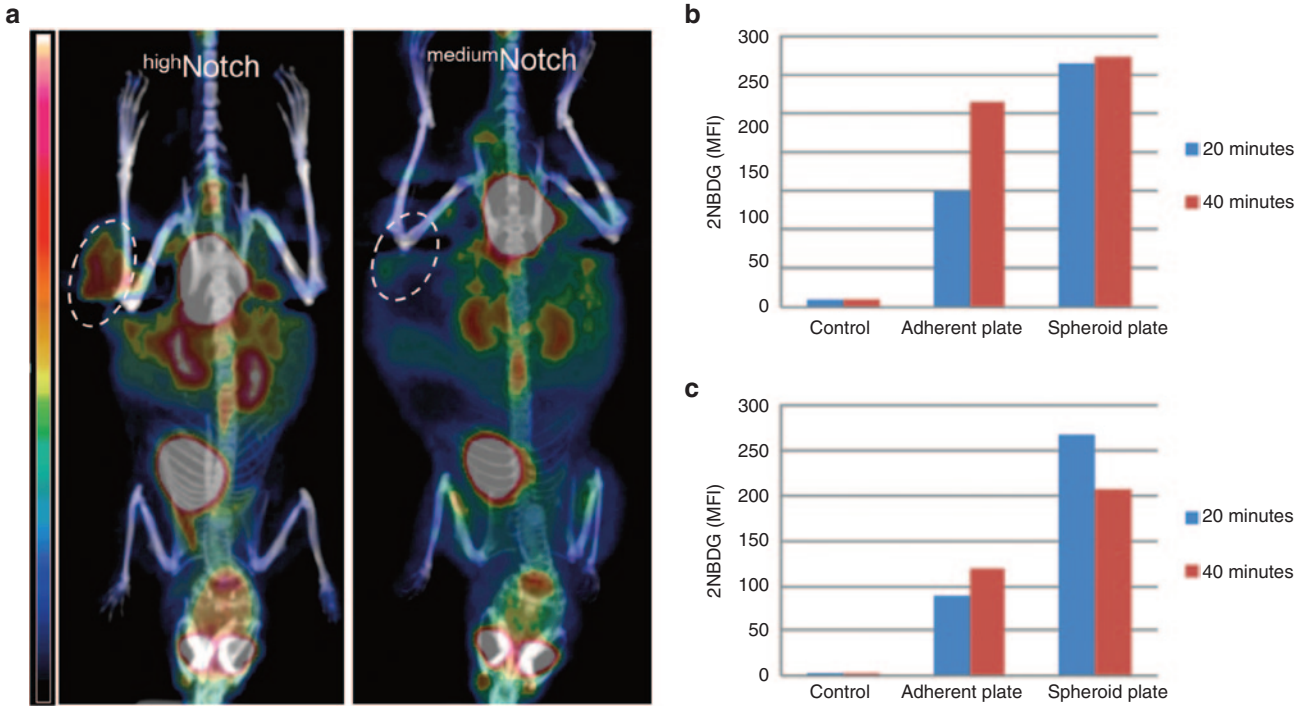

Figure 3 Tumors with hyperactive Notch signaling show enhanced glucose uptake. (**a**) Representative ^{18}F-FDG PET images of mice 5 weeks after grafting with MCF7 cells engineered to express elevated or medium levels of Notch (tumor areas are circled). Scale bar 3E-1-5E0. (**b,c**) Cell populations enriched for cancer stem cells have enhanced glucose uptake. FACS analyses of naive MDA-MB-231 (**b**) and MCF7 (**c**) cells grown as adherent cells (adherent plate) or nonadherent spheroids (spheroid plate) incubated with fluorescently labeled deoxyglucose, 2NBDG, for 20 and 40 minutes. 2NBDG is displayed as mean fluorescent intensity. Cells grown as spheroids have enhanced glucose uptake. Shown is a representative graph of one out of three experiments.

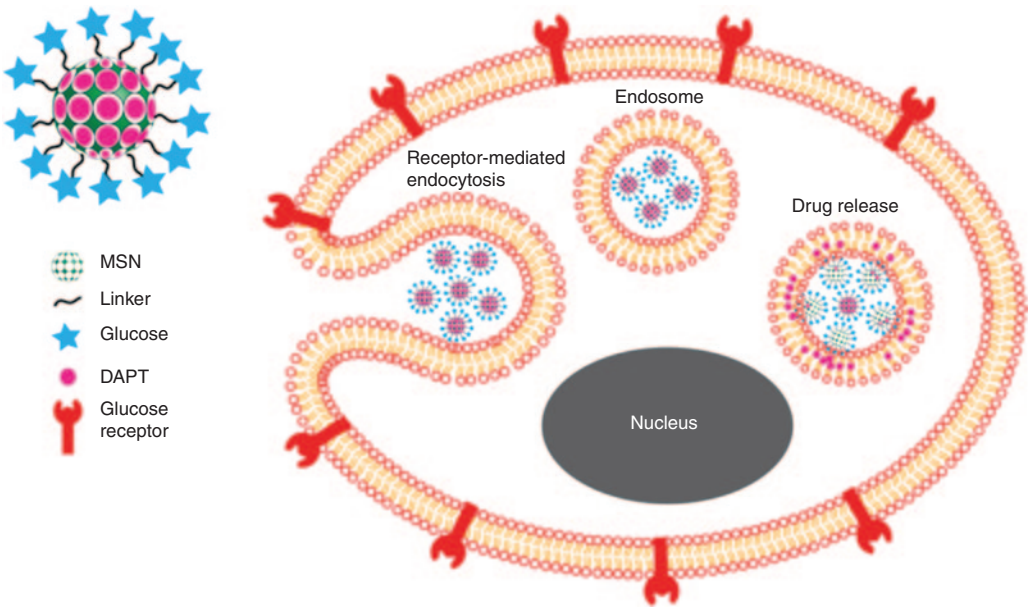

Figure 4 Schematic presentation of the nanoparticle design. Elevated Notch signaling activity promotes the glycolytic phenotype; is important for self-renewal of cancer stem cells and supports estrogen-independent growth in estrogen positive breast cancer. Glycolytic cancer cells and cancer stem cells express glucose receptors on the surface. For efficient delivery of γ-secretase inhibitors (GSI), potent inhibitors of Notch activity, to glycolytic cancer stem cells we functionalized mesoporous silica particles with glucose moieties to target glucose receptors. The hydrophobic GSI is released from the particles and diffuses in the endosomal and cell membranes where it inhibits the γ-secretase, which is responsible for activating Notch signaling by proteolytic processing of the receptor. The glucose entities were linked to the particle to allow the glucose to interact with the glucose import systems, the glucose receptors, of the cells.

when they were functionalized with glucose entities (MSN-PEI versus MSN-PEI-GA$_{org}$; MSN versus MSN-G), although the increase was not significant for the particles lacking PEI and with direct glucose entity conjugation (MSN-G) (**Figure 5a,b**). However, it is well established that particles adsorbed to the outer cell membrane and not internalized by the cells could contribute to the fluorescent signal as determined by FACS. Therefore, The cellular uptake of the particles was further investigated by confocal microscopy (**Figure 5c**). Whereas MSN-G particles displayed an intracellular vesicular pattern, the nonglucose-tagged

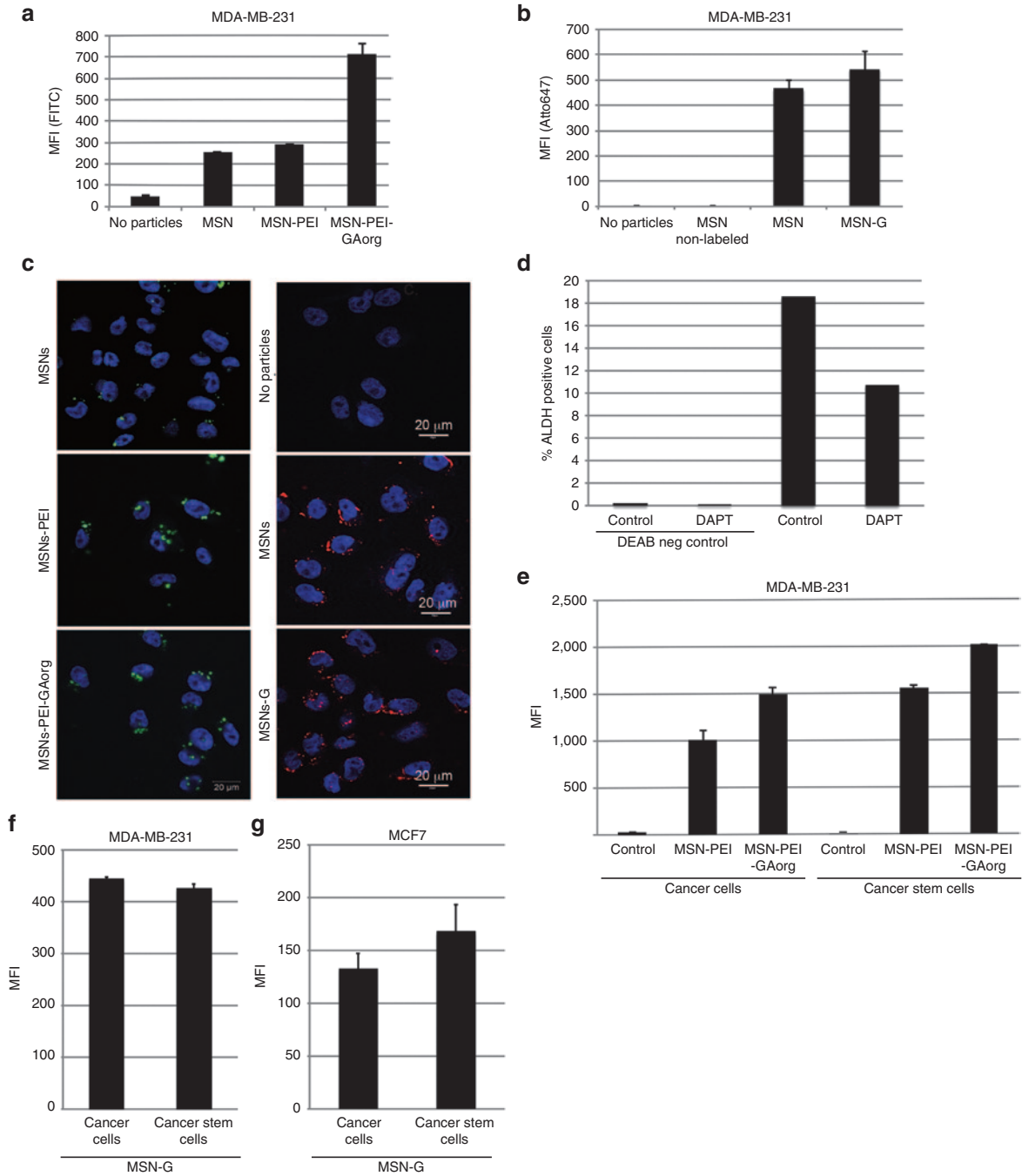

Figure 5 Uptake of glucose-functionalized particles in MDA-MB-231 cancer and cancer stem cells. MDA-MB-231 cells were incubated with the different particles at a concentration of 20 µg /ml particles for 4 hours after which they were collected and particle uptake was analyzed by flow cytometry (**a**,**b**). The graphs show uptake of differently functionalized mesoporous silica particles (MSN) in MDA-MB-231 breast cancer cells. The different particles used are denoted on the x-axis. (**c**) The confocal images show cell internalization of MSN- G nanoparticles in MDA-MB-231 cells, while MSN particles are rather located close to the outer cell membrane. (**d**) The graph show % of cancer stem cells in control and DAPT (5 µg/ml, 24 hours) treated MDA-MB-231 cells, as determined by ALDH activity by FACS analyses. (**e**) Uptake of MSN-PEI and MSN-PEI-GAorg in cancer cells and cancer stem cells. (**f**,**g**) Uptake of MSN-G in cancer cells and cancer stem cells in MDA-MB-231 (**f**) and MCF7 cells (**g**) as determined by FACS (**f**). DEAB, diethylaminobenzaldehyde. The graphs show the result of three independent experiments, with three experimental repetitions within each experiment. FITC, fluorescein isothiocyanate.

MSN particles mostly accumulated in larger aggregates at the cell boarder, further supporting enhanced intracellular delivery by glucose functionalization. On the contrary, the PEI-functionalized particles displayed a more similar cellular distribution regardless the glucose functionalization (**Figure 5c**). Further, functionalization of particles with glucose moieties significantly enhanced uptake in MDA-MB-231 cancer cells as compared to the uptake in MCF10 mammary epithelial cells (**Supplementary Figure S6b,c**). Nonfunctionalized particles were internalized to the same degree by cancer and healthy cells. Of note, PEI-functionalization per se enhanced uptake in MDA-MB-231 cancer cells as compared to mammary epithelial cells MCF10 (**Supplementary Figure S6b**).

We next wanted to analyze uptake in CSCs. The CSC population was identified by aldehyde dehydrogenase-1 (ALDH1) activity in the cells using the ALDEFLUOR kit (Stem Cell Technologies, Cambridge, UK). Pharmacological inhibition of Notch by DAPT (N-[N-(3,5-difluorophenacetyl)-L-alanyl]-S-phenylglycine t-butyl ester) for 24 hours prior to the analyses reduced the percentage of cells displaying ALDH1 activity, in line with the importance of Notch signaling for stem cell maintenance and renewal (**Figure 5d** and **Supplementary Figure S7a**). Both cancer cells and CSCs demonstrated efficient uptake of the MSN-PEI-GA_{org} particles, with CSCs demonstrating increased uptake as compared to cancer cells (**Figure 5e**). CSCs also displayed enhanced uptake of the PEI-functionalized particles (MSN-PEI) (**Figure 5f**). By contrast, there was no significant increase in the uptake of the MSN-G particles in MDA-MB-231 CSCs as compared to cancer cells. However, in the less glycolytic MCF7 cells, where the CSC population demonstrated significantly enhanced glucose uptake as compared to the cancer cell population (**Figure 3c**), glucose functionalization increased the uptake of these particles in CSCs. Taken together, these data indicate that glucose targeting facilitates uptake in cancer cells and CSCs in accordance with the glycolytic phenotype of the cells.

To verify tumor targeting *in vivo*, we transplanted 3×10^6 glycolytic MDA-MB-231 cells orthotopically in the mammary glands in female NOD SCID mice. When the tumors reached ~100 mm^3, 20 mg/kg MSN or MSN-G particles, labeled with Atto647 for *in vivo* imaging, were injected in the tail vein. Both MSN and MSN-GA particles accumulated in the tumors (**Figure 6a**), albeit with different kinetics. For quantification of fluorescence intensity in the tumors, see **Figure 6b**.

GSI loaded glucose-functionalized MSNs reduce the cancer stem cell pool *in vivo*

To inhibit the Notch signaling pathway, we loaded the MSNs with the GSI, DAPT. The DAPT loading degree, µg DAPT per mg particles, for each set of particles was determined by high-performance liquid chromatography, and varied between 13 and 73 µg/mg between the different particles (**Supplementary Figure S5**). The ability of particles to inhibit the Notch signaling pathway and reduce the CSC pool was tested *in vitro* by treating adherent and spheroid MDA-MB-231 cells with DAPT and DAPT-loaded particles. Spheroids displayed higher ALDH1 activity in accordance with the enrichment of CSCs in spheroid cultures as compared to adherent cultures (**Supplementary Figure S7a**). Cells treated with free DAPT 5 or 50 µg/ml particles (note variable DAPT concentration) for 24 hours demonstrated reduced ALDH activity indicating a loss of CSC characteristics (**Supplementary Figure S7a**). The data demonstrated that inhibition of Notch by DAPT eliminates CSCs *in vitro*.

To verify the therapeutic efficacy and ability to target the CSCs *in vivo*, we utilized the chorioallantoic membrane (CAM) of a chick embryo as a tumor model.[39] 1×10^6 MDA-MB-231 cells were transplanted on the CAM on embryonic day 8, E8. From E8, particles were administered topically on the tumor once a day until day E13, when the tumor was explanted, weighed and dissociated, and analyzed by FACS. For the *in vivo* experiments, the particle concentration was adjusted such that the daily DAPT dose was 1 µg/tumor. Cancer cells and residual CAM cells were identified based on light scattering, whereas the CSCs were identified based on ALDH activity (**Supplementary Figure S7b**). The average number of events, *i.e.*, number of cancer cells, CSCs and CAM cells per treatment is shown in **Supplementary Figure S7c**.

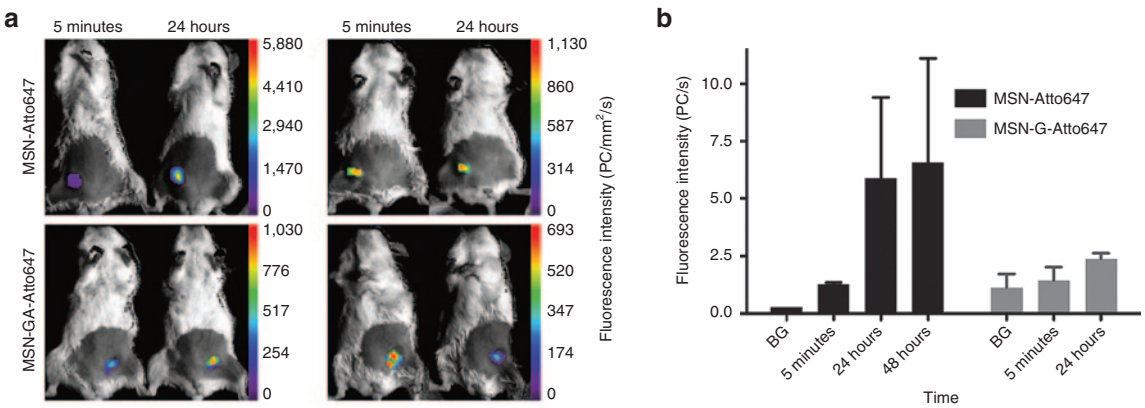

Figure 6 Uptake of glucose-functionalized (GA) particles in MDA-MB-231 tumors *in vivo*. (**a**) Accumulation of mesoporous silica particles (MSN) and MSN-GA particles in orthotopic MDA-MB-231 tumors in NSG mice after intravenous injection of 20 mg/kg particles. Tumors were implanted either in the left or the right mammary inguinal glands and distributed into two groups to receive either MSN or MSN-GA particles. Tumor accumulation was analyzed with Optix MX3 Small Animal Molecular Imager system (ART Inc) and the Optiview software (Versions 1.04 and 2.02; ART). The figure shows images of two mice injected with MSN particles (upper images) and two mice injected with MSN-GA particles (lower images) at the day of injection and the following day (24 hours). (**b**) The graphs show quantification of fluorescent intensity.

For further analyses, the number of cancer cells and CSCs per mg tissue was denoted.

The analyses demonstrated a slight but significant decrease in number of cancer cells per mg tissue upon treatment with DAPT-loaded particles as compared to particles controls (**Supplementary Figure S8**). However, no significant difference in the number of CSCs was observed (**Supplementary Figure S8**). The data is in agreement with the insignificant difference in uptake of particles between cancer cells and CSCs (**Figure 5**).

A similar approach was used to evaluate therapeutic efficacy of the other set of particles where the glucose moiety was linked to the particle through PEI. Treatment with free DAPT or DAPT-loaded particles significantly reduced number of cancer cells per mg/tissue (**Figure 7a**). In addition, the number of CSCs per mg/tissue was significantly reduced in tumors treated with free DAPT, MSN-PEI-DAPT, MSN-PEI-GA_{org}-DAPT as compared to vehicle or nonloaded particle controls (**Figure 7b**). Interestingly, while the number of cancer cells/mg tissue was decreased as compared to the control for both non-loaded MSN-PEI and MSN-PEI-GA_{org}, the number of cancer stem cells, especially in the case of MSN-PEI-GA_{org}, was higher than the control, which could suggest that these particles in their native state (without drug load) may boost the proliferation rate of the stem cells. These results are in line with *in vivo* results presented in Mamaeva *et al.*,[38] where intravenous administration of empty MSN-PEI-FA particles leads to enhanced Notch signaling, and enhanced tumor growth as compared to the control. Our data suggest that the surface charge of the particles (cationic/anionic) could be an important factor for influencing such background activity. In any case, free DAPT and DAPT-loaded particles reduced the number of CSCs. When the data were presented as fold reduction of CSCs as compared to the respective controls, it was evident that the glucose functionalized, DAPT-containing particles had the greatest effect on reducing CSCs. Taken together, we demonstrated that MSNs loaded with DAPT, especially when surface functionalized with glucose in combination with a cationic surface charge, efficiently targets and reduces the CSC population within a tumor.

DISCUSSION

Here, we demonstrate that Notch signaling is necessary for CSC self-renewal, therapy resistance and a metabolic switch to a glycolytic phenotype in breast cancer cells. We also show that CSCs display a glycolytic phenotype, and show enhanced glucose uptake as compared to cancer cells. Estrogen-independent breast cancer cells have higher Notch activity than estrogen-dependent cancer cells, and Notch signaling has been proposed to promote

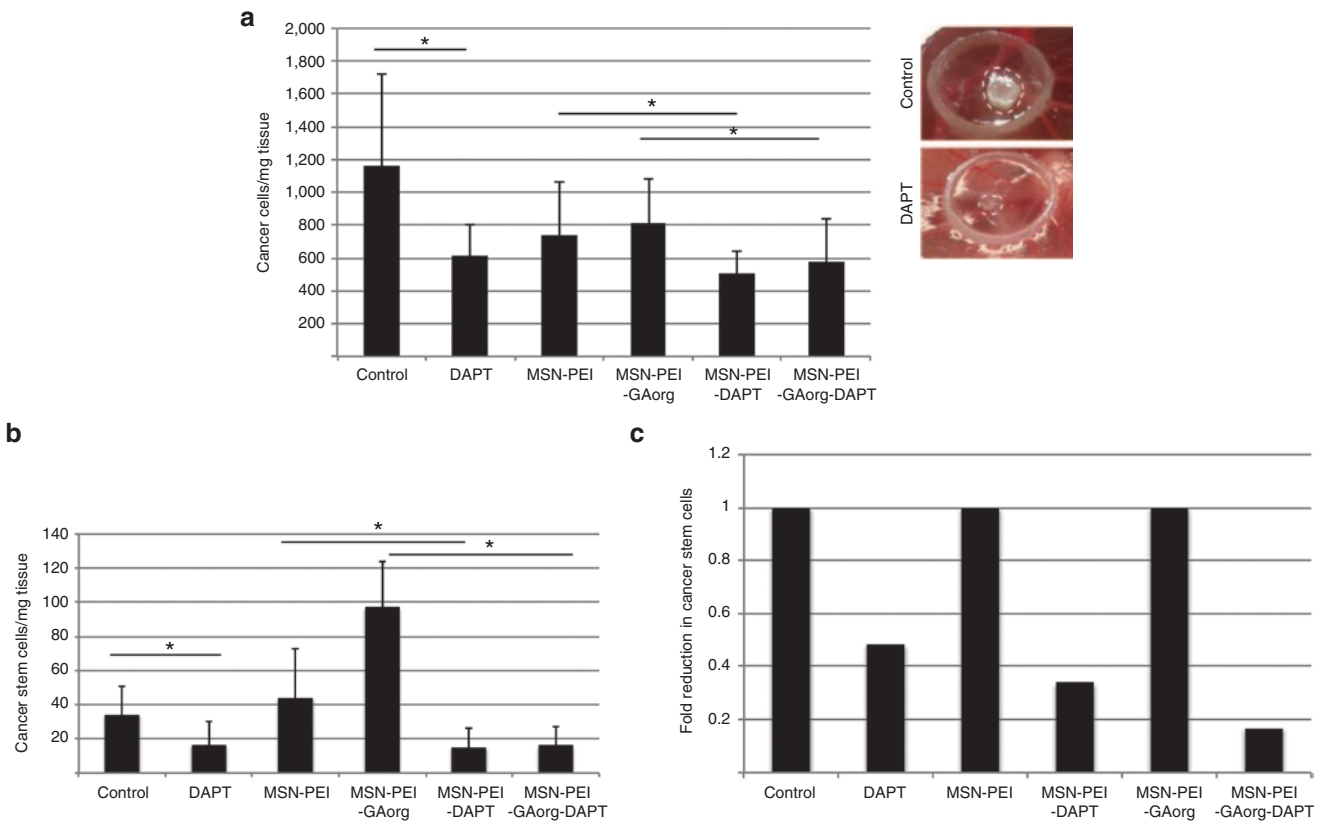

Figure 7 Efficacy of glucose-functionalized polymer coated particles in MDA-MB-231 tumors *in vivo*. MDA-MB-231 cells were transplanted on chorioallantoic membrane (CAM) and treated with DAPT loaded or empty particles. The particle concentration was adjusted based on the DAPT loading degree (**Supplementary Figure S5**), such that the DAPT amount was 1 µg. Treatment (1 µg in 30 µl HEPES) was applied topically every day from the day of transplantation. After 5 days, the tumor was removed and the tissue was dissected and number of cancer cells (**a**, left) and cancer stem cells (**b**) was determined by FACs analyses. The graphs denote number of cells/mg of dissected tissue. (**a**, right) Photograph of MDA-MB-231 tumors on CAM treated with vehicle (control) or DAPT. (**c**) The graph demonstrates the fold decrease in number of cancer stem cells per mg of tissue as correlated to the number in the respective control situation, which has been given the value 1. Control denotes untreated tumors and DAPT denotes tumors treated with DAPT-loaded nanoparticles. Statistical significance is denoted by $*P \leq 0.05$, $**P \leq 0.01$. HEPES, 4-(2-hydroxyethyl)-1-piperazineethanesulfonic acid.

estrogen-independent growth and resistance to estrogen-targeted therapies such as Tamoxifen.[19,23,26,44,45] We demonstrate that enforced Notch activation in estrogen-dependent cell lines promotes estrogen-independent growth *in vivo*, further strengthening the notion that Notch mediates hormone- and chemoresistance. CSCs have also been demonstrated to be chemoresistant and we link Notch signaling to CSCs estrogen-independent growth. Our data suggest that Notch inhibitors should be clinically evaluated in hormone-resistant breast cancers to enhance therapeutic efficacy, and to combat the CSC pool to prevent later recurrence. The importance of Notch signaling in CSC resistance is in line with recent data demonstrating that Notch promotes recurrence after Her2-targeted therapy.[17]

Despite the availability of efficient Notch inhibitors,[24,44] the requirement of Notch in maintaining homeostasis in most tissues prevents the use of Notch inhibitors, and locally retained drug delivery is needed. Nanoparticles are well suited for targeted and controlled drug delivery. We have previously developed MSNs for tumor-targeted delivery of Notch inhibitors and demonstrated enhanced therapeutic efficacy and reduced side effects in preclinical tumor models of breast cancer.[38] Here, we developed the platform further and utilized the specific metabolic profile of CSCs for efficient delivery of the Notch inhibitor DAPT to CSCs. DAPT-loaded bare and glucose-functionalized particles are efficiently internalized by CSC, reduce the CSC pool and inhibit tumor growth *in vitro* and *in vivo*.

Our data indicate that the surface charge of the MSNs influence uptake and targetability of the particles. Efficient targeting was observed for the glucose-tagged MSN-PEI particles, while a moderate targetability was observed for the anionic MSN-G particles. This difference is ascribed to the often observed more efficient uptake of cationic MSNs as compared to anionic MSNs,[46] as an efficient electrostatically driven attachment to the negatively charged cell membrane is suggested to kinetically enhance uptake, both in the presence and absence of targeting ligands. It has been suggested that cationic particles can induce local nanoscale disruptions in the cell membrane, which enhances uptake.[47] The enhanced uptake of cationic MSNs in CSCs as compared to that observed for cancer cells is in agreement with data reported by Chung *et al*., demonstrating higher uptake of MSNs by mesenchymal stem cells (MSCs) as compared to 3T3-L1 cells.[48] Further, Lee *et al*.[49] showed that MSCs exhibited a clearly more negative surface charge than differentiated cells. If this is true also for breast CSCs, this would explain the enhanced uptake of the cationic particles by these cells, and the more efficient DAPT delivery observed for the PEI-functionalized cationic particles as compared to the anionic counterparts. We do further not exclude the contribution of a more efficient retention of drug in the PEI-coated particles,[43] where PEI could act as a so-called molecular gate,[41] leading to more efficient intracellular drug delivery. As the particle diameters in the two cases are relatively similar, we do exclude particle size differences as the main reason for this observation. We also observed a higher number of CSCs in the tumors treated with nonloaded strongly cationic particles, which suggests that surface charge may be crucial for the effect of particles on stem cell self renewal and proliferation. This notion is in line with data in Chung *et al*.[48] demonstrating that that there is a cationic charge threshold above which proliferation is induced. This effect was not observed for particles with moderately cationic or anionic surface charge, and not in DAPT-loaded particles where drug release and effect coincide with particle degradation.[38–41] Thus, our results in combination with other studies suggest that the MSN surface charge is indeed a decisive factor for stem cell proliferation rate, and care should be taken to not use too strongly cationic MSNs when aiming for cancer therapy-related applications. We can also relate this enhanced proliferation rate to the enhanced Notch levels induced by high concentrations of empty cationic particles demonstrated by us.[38] Therefore, nanoparticle-influences on Notch levels are suggested to be useful evaluation criteria *in vitro* in future nanoparticle developments aiming at CSC-targeted therapies. A moderately cationic surface charge is suggested to be optimal, as the targetability was clearly enhanced for the cationic particles as compared to the anionic particles. However, the anionic glucose-functionalized MSNs were demonstrated to accumulate in the tumor area immediately after injection in the mouse model, and the particles were retained in the tumor area 1 day postinjection. Control particles void of glucose, on the other hand, showed a very low level of early tumor accumulation, but were observed to accumulate in the tumor area with time. These results demonstrate the value of glucose-functionalization also for the anionic MSN particles, although the level of targetability was limited *in vitro*. To which extent the early accumulation of MSN-G particles in the tumor area *in vivo* can be related to different extents of opsonization or to active targeting of the MSN-G particles in comparison to the control particles remains to be evaluated in future studies.

Our approach presents dual targeting of CSCs utilizing both the dependence of a specific stem cell pathway, Notch, for CSC function, and the specific metabolic profile of CSC to develop an efficient drug delivery platform for cancer treatment with a specific focus on eliminating the CSC population. The glycolytic phenotype of cancer cells have long been utilized for PET imaging and diagnostics in cancer, but has yet to be employed in targeted cancer stem cell therapy in the clinic although attempts to target cancer cell metabolisms has gained tremendous interest and several approaches are currently pre-clinically and clinically evaluated.[50,51] We demonstrate that the CSCs also display a unique metabolic profile, which can be used to enhance therapeutic efficacy by targeting and eliminating the CSC pool. We demonstrate successful targeting and elimination of CSCs achieved by elucidation of molecular pathways necessary for CSC survival and resistance, and the identification of specific characteristics of CSCs and by developing a nanoparticle platform to target these characteristics of CSCs. Our data demonstrate that combining in depth understanding of CSC biology, and the development of drug delivery platforms has the potential to open up new possibilities for therapeutic intervention and enhance the success of current treatments.

MATERIALS AND METHODS

Cell culture. The cells used to generate stable cell lines were purchased from ATCC (Manassas, VA) and validated in 2009. The stable cell lines were generated at Karolinska Insitute and at Turku Centre for Biotechnology. Naive MDA-MB-231 and MCF7 cells used were purchased in 2010 and 2013 from ATCC. Human breast cancer cell lines MCF7 (including stable and inducible cell lines) and MDA-MB-231 were grown in Dulbecco's

modified eagle's medium (Sigma D6171) supplemented with 10% fetal calf serum, L-glutamine, 25,000 units penicillin/25 mg streptomycin, nonessential amino acids, and sodium pyruvate. Spheroid cells were cultured on bacterial plates and were grown in Dulbecco's modified eagle's medium supplemented with 25 ng/ml basic fibroblast growth factor, 25 ng/ml epithelial growth factor, 1× B-27, 1 mmol L-glutamine, and 25,000 units penicillin/25 mg streptomycin. Stable cell lines were selected with puromycin (1 µg/ml). Notch activity was blocked by addition of 5 µg/ml γ-secretase inhibitor **N**-[**N**-(3,5-difluorophenacetyl)-L-alanyl]-**S**-phenylglycine **t**-butyl ester (DAPT; Calbiochem). Inducible Tet-on cell lines designated MCF7-EGFP and MCF7-N1ΔEGFP were induced by addition of 1 µg/ml doxycyclin. For particle handling and analyses of cellular uptake, see ref. [38].

Glucose uptake. Glucose uptake was measured using 2-NBDG (2-(*N*-(7-nitrobenz-2-oxa-1,3-diazol-4- yl)amino)-2-deoxyglucose) fluorescent probes (Invitrogen). MCF-7 cells were incubated in medium containing 100 µmol/l probe for 20 minutes. Cells were then washed twice in phosphate-buffered saline (PBS), trypsinized, pelleted, and resuspended in PBS followed by flow cytometry analysis using BD FACSCalibur running BD CellQuest PRO v.5.1.1 (BD Biosciences, Heidelberg, Germany).

Nanoparticle synthesis, characterization, and* in vitro *evaluation; preclinical imaging. See **Supplementary Materials and Methods**.

Tumor xenografts. Animal experiments were conducted in accordance with the Institutional animal care policies of the University of Turku and Åbo Akademi University and/or approved by the Norwegian Animal Research Authority and performed in accordance with The European Convention for the Protection of Vertebrates Used for Scientific Purposes. Optical imaging studies (see **Supplementary Data**) were performed on female NOD/SCID IL2rγ^{null} (NSG) mice (Vivarium, University of Bergen). For additional information, refer to **Supplementary Materials and Methods**.

Histological analysis and immunohistochemistry. Paraffin embedding, sectioning, and hematoxylin-eosin staining was performed in the Department of Pathology and Forensic Medicine, University of Turku (special thanks to Sinikka Collanus). Immunohistochemistry was carried out with standard techniques, using commercial antibodies for Ki-67, CD44, CK5/6, ER and secondary antibody (Dako Cytomation EnVision System Copenhagen, Denmark). The reaction products were visualized applying DAB solution (Dako Cytomation Liquid DAB Substrate Chromogen System). Sections were then counterstained with Mayer's hematoxylin. Negative controls were obtained by omission of the primary antibody. A board-certified pathologist reviewed slides in blind.

Chicken chorioallantoic membrane assay. Fertilized eggs are provided by Munax Oy (Laitila, Finland) and placed oval end upwards in a thermostat incubator at 37 °C at 65% relative humidity with 3-day rotation after cleaning with 70% ethanol. Eggs are turned upside down and a small hole is opened on the pointed end. 1 million cultured cells are mixed with 10 µl cell media and 10 µl Matrigel and xenografted on top of the CAM inside the plastic ring (7 mm diameter) on the eighth day of egg development. Xenografted tumors are incubated for 24 hours to attach to the membrane. Nanoparticle concentration is adjusted to acquire 1 µg DAPT for each treatment, and particles are sonicated in 4-(2-hydroxyethyl)-1-piperazineethanesulfonic acid for 20 minutes before topical treatment, performed over 6 days.

The tumors are collected on day 13 and washed with PBS at +4 °C. Wet weights of tumors are quantified and minced for enzyme treatment. Corning Dispase is diluted with PBS to a 2 U/ml concentration and tumors are incubated at 37 °C, 5% CO_2 for 2 hours. The suspension is filtered through a silk filter (70 µm mesh size) and washed twice with PBS at 1,000 rpm for 5 minutes. ALDEFLUOR assay is used for evaluation and identification of stem cells, according to the manufacturer's instructions. Briefly, cells derived from tumors are redissolved in 1 ml ALDEFLUOR Assay Buffer at room temperature. Test samples are prepared with 5 µl ALDEFLUOR Reagent and negative control samples are prepared with additional 5 µl of ALDEFLUOR DEAB Reagent (diethylaminobenzaldehyde) to inhibit the ALDEFLUOR and acquire background values; samples are then incubated for 50 minutes at 37 °C, 5% CO_2. Following incubation, samples are centrifuged at 1,000 rpm for 5 minutes and pellets are resuspended in 0.4 ml ALDEFLUOR Assay Buffer and stored on ice for FACS. Flow cytometry analysis is performed using FACSCalibur (BD Sciences) with an FL1 channel (Ex. 488 nm/Em. 530 nm). 100,000 cells are collected from each sample for analysis.

SUPPLEMENTARY MATERIAL

Figure S1. Glycolysis was analyzed in dnCSL MCF7 and untreated MDA-MB-231 by measuring the extracellular acidification rate (ECAR) by use of a Seahorse XFe96 Analyzer.
Figure S2. TEM images and overview of nanoparticle characteristics.
Figure S3. Schematic presentation of synthesis and characteristics of MSN-G.
Figure S4. Thermogravimetric analyses and optical analyses of fluorescent particles.
Figure S5. Quantification of the DAPT load in particles.
Figure S6. Uptake of glucose functionalized particles in MDA-MB-231 cancer cells and cancer stem cells, in healthy MCF10 mammary epithelial cells and *in vivo*.
Figure S7. Notch inhibition by DAPT eliminates the cancer stem cell population *in vitro* and *in vivo.*
Figure S8. MDA-MB-231 cells were transplanted on CAM and treated with DAPT loaded or empty particles.
Data
Materials and methods

ACKNOWLEDGMENTS

This work was supported by the Academy of Finland grants 218062 (C.S.) 260599 (E.Ö., D.D., and J.M.R.) and Sigrid Juselius Foundation and Cancer Society of Finland (C.S.). R.N. was supported by the Swedish Cultural Foundation of Finland, Svensk-österbottniska samfundet, K. Albin Johansson foundation, Liv och Hälsa Foundation. S.L. was supported by the Swedish Cultural Foundation of Finland, Magnus Ehrnrooth Foundation, Waldemar von Frenckell Foundation, K. Albin Johansson foundation, the Swedish Research Council, EU (ITN NotchIT). M.B. was supported by Ulm University funding. E.M. was supported by the Norwegian Cancer Society (grant number 732200), the Western health board of Norway (Helse Vest; grant numbers 911182 and 911789), and the Bergen Research Foundation. The Cell Imaging Core at the Turku Center of Biotechnology is thanked for access to infrastructure and technical assistance. The in vivo fluorescence imaging was performed at the Molecular Imaging Centre (MIC), University of Bergen, and Mireia Mayoral Safont is thanked for her technical assistance. The authors declare that they have no conflict of interest.

REFERENCES

1. Al-Hajj, M, Wicha, MS, Benito-Hernandez, A, Morrison, SJ and Clarke, MF (2003). Prospective identification of tumorigenic breast cancer cells. *Proc Natl Acad Sci USA* **100**: 3983–3988.
2. Bonnet, D and Dick, JE (1997). Human acute myeloid leukemia is organized as a hierarchy that originates from a primitive hematopoietic cell. *Nat Med* **3**: 730–737.
3. O'Brien, CA, Pollett, A, Gallinger, S and Dick, JE (2007). A human colon cancer cell capable of initiating tumour growth in immunodeficient mice. *Nature* **445**: 106–110.
4. Reya, T, Morrison, SJ, Clarke, MF and Weissman, IL (2001). Stem cells, cancer, and cancer stem cells. *Nature* **414**: 105–111.
5. Singh, SK, Hawkins, C, Clarke, ID, Squire, JA, Bayani, J, Hide, T *et al.* (2004). Identification of human brain tumour initiating cells. *Nature* **432**: 396–401.
6. Dean, M, Fojo, T and Bates, S (2005). Tumour stem cells and drug resistance. *Nat Rev Cancer* **5**: 275–284.
7. LaBarge, MA (2010). The difficulty of targeting cancer stem cell niches. *Clin Cancer Res* **16**: 3121–3129.
8. Plaks, V, Kong, N and Werb, Z (2015). The cancer stem cell niche: how essential is the niche in regulating stemness of tumor cells? *Cell Stem Cell* **16**: 225–238.
9. Shibuya, K, Okada, M, Suzuki, S, Seino, M, Seino, S, Takeda, H *et al.* (2015). Targeting the facilitative glucose transporter GLUT1 inhibits the self-renewal and tumor-initiating capacity of cancer stem cells. *Oncotarget* **6**: 651–661.

10. Ntziachristos, P, Lim, JS, Sage, J and Aifantis, I (2014). From fly wings to targeted cancer therapies: a centennial for notch signaling. *Cancer Cell* **25**: 318–334.
11. Hori, K, Sen, A and Artavanis-Tsakonas, S (2013). Notch signaling at a glance. *J Cell Sci* **126**(Pt 10): 2135–2140.
12. Reedijk, M, Pinnaduwage, D, Dickson, BC, Mulligan, AM, Zhang, H, Bull, SB *et al.* (2008). JAG1 expression is associated with a basal phenotype and recurrence in lymph node-negative breast cancer. *Breast Cancer Res Treat* **111**: 439–448.
13. Takebe, N, Miele, L, Harris, PJ, Jeong, W, Bando, H, Kahn, M *et al.* (2015). Targeting Notch, Hedgehog, and Wnt pathways in cancer stem cells: clinical update. *Nat Rev Clin Oncol* **12**: 445–464.
14. Muellner, MK, Uras, IZ, Gapp, BV, Kerzendorfer, C, Smida, M, Lechtermann, H *et al.* (2011). A chemical-genetic screen reveals a mechanism of resistance to PI3K inhibitors in cancer. *Nat Chem Biol* **7**: 787–793.
15. Dong, Y, Li, A, Wang, J, Weber, JD and Michel, LS (2010). Synthetic lethality through combined Notch-epidermal growth factor receptor pathway inhibition in basal-like breast cancer. *Cancer Res* **70**: 5465–5474.
16. Martz, CA, Ottina, KA, Singleton, KR, Jasper, JS, Wardell, SE, Peraza-Penton, A *et al.* (2014). Systematic identification of signaling pathways with potential to confer anticancer drug resistance. *Sci Signal* **7**: ra121.
17. Abravanel, DL, Belka, GK, Pan, TC, Pant, DK, Collins, MA, Sterner, CJ *et al.* (2015). Notch promotes recurrence of dormant tumor cells following HER2/neu-targeted therapy. *J Clin Invest* **125**: 2484–2496.
18. Pannuti, A, Foreman, K, Rizzo, P, Osipo, C, Golde, T, Osborne, B *et al.* (2010). Targeting Notch to target cancer stem cells. *Clin Cancer Res* **16**: 3141–3152.
19. Rizzo, P, Miao, H, D'Souza, G, Osipo, C, Song, LL, Yun, J *et al.* (2008). Cross-talk between notch and the estrogen receptor in breast cancer suggests novel therapeutic approaches. *Cancer Res* **68**: 5226–5235.
20. Sahlgren, C, Gustafsson, MV, Jin, S, Poellinger, L and Lendahl, U (2008). Notch signaling mediates hypoxia-induced tumor cell migration and invasion. *Proc Natl Acad Sci USA* **105**: 6392–6397.
21. Mani, SA, Guo, W, Liao, MJ, Eaton, EN, Ayyanan, A, Zhou, AY *et al.* (2008). The epithelial-mesenchymal transition generates cells with properties of stem cells. *Cell* **133**: 704–715.
22. Landor, SK, Mutvei, AP, Mamaeva, V, Jin, S, Busk, M, Borra, R *et al.* (2011). Hypo- and hyperactivated Notch signaling induce a glycolytic switch through distinct mechanisms. *Proc Natl Acad Sci USA* **108**: 18814–18819.
23. Takebe, N, Nguyen, D and Yang, SX (2014). Targeting notch signaling pathway in cancer: clinical development advances and challenges. *Pharmacol Ther* **141**: 140–149.
24. Andersson, ER and Lendahl, U (2014). Therapeutic modulation of Notch signalling–are we there yet? *Nat Rev Drug Discov* **13**: 357–378.
25. van Es, JH, van Gijn, ME, Riccio, O, van den Born, M, Vooijs, M, Begthel, H *et al.* (2005). Notch/gamma-secretase inhibition turns proliferative cells in intestinal crypts and adenomas into goblet cells. *Nature* **435**: 959–963.
26. Rizzo, P, Osipo, C, Foreman, K, Golde, T, Osborne, B and Miele, L (2008). Rational targeting of Notch signaling in cancer. *Oncogene* **27**: 5124–5131.
27. Yan, M, Callahan, CA, Beyer, JC, Allamneni, KP, Zhang, G, Ridgway, JB *et al.* (2010). Chronic DLL4 blockade induces vascular neoplasms. *Nature* **463**: E6–E7.
28. Chiorean, EG, LoRusso, P, Strother, RM, Diamond, JR, Younger, A, Messersmith, WA *et al.* (2015). A phase I first-in-human study of enoticumab (REGN421), a fully human delta-like ligand 4 (Dll4) monoclonal antibody in patients with advanced solid tumors. *Clin Cancer Res* **21**: 2695–2703.
29. Markman, JL, Rekechenetskiy, A, Holler, E and Ljubimova, JY (2013). Nanomedicine therapeutic approaches to overcome cancer drug resistance. *Adv Drug Deliv Rev* ***65***: 1866–1879.
30. Orza, A, Casciano, D and Biris, A (2014). Nanomaterials for targeted drug delivery to cancer stem cells. *Drug Metab Rev* **46**: 191–206.
31. Saenz del Burgo, L, Pedraz, JL and Orive, G (2014). Advanced nanovehicles for cancer management. *Drug Discov Today* **19**: 1659–1670.
32. Allen, TM and Cullis, PR (2013). Liposomal drug delivery systems: from concept to clinical applications. *Adv Drug Deliv Rev* ***65***: 36–48.
33. Venditto, VJ and Szoka, FC Jr (2013). Cancer nanomedicines: so many papers and so few drugs! *Adv Drug Deliv Rev* ***65***: 80–88.
34. Kraft, JC, Freeling, JP, Wang, Z and Ho, RJ (2014). Emerging research and clinical development trends of liposome and lipid nanoparticle drug delivery systems. *J Pharm Sci* **103**: 29–52.
35. Bertrand, N, Wu, J, Xu, X, Kamaly, N and Farokhzad, OC (2014). Cancer nanotechnology: the impact of passive and active targeting in the era of modern cancer biology. *Adv Drug Deliv Rev* ***66***: 2–25.
36. Mamaeva, V, Sahlgren, C and Lindén, M (2013). Mesoporous silica nanoparticles in medicine–recent advances. *Adv Drug Deliv Rev* ***65***: 689–702.
37. Rosenholm, JM, Mamaeva, V, Sahlgren, C and Lindén, M (2012). Nanoparticles in targeted cancer therapy: mesoporous silica nanoparticles entering preclinical development stage. *Nanomedicine (Lond)* **7**: 111–120.
38. Mamaeva, V, Rosenholm, JM, Bate-Eya, LT, Bergman, L, Peuhu, E, Duchanoy, A *et al.* (2011). Mesoporous silica nanoparticles as drug delivery systems for targeted inhibition of Notch signaling in cancer. *Mol Ther* **19**: 1538–1546.
39. Wittig, R, Rosenholm, JM, von Haartman, E, Hemming, J, Genze, F, Bergman, L *et al.* (2014). Active targeting of mesoporous silica drug carriers enhances γ-secretase inhibitor efficacy in an *in vivo* model for breast cancer. *Nanomedicine (Lond)* **9**: 971–987.
40. Böcking, D, Wiltschka, O, Niinimäki, J, Shokry, H, Brenner, R, Lindén, M *et al.* (2014). Mesoporous silica nanoparticle-based substrates for cell directed delivery of Notch signalling modulators to control myoblast differentiation. *Nanoscale* **6**: 1490–1498.
41. Rosenholm, JM, Peuhu, E, Eriksson, JE, Sahlgren, C and Lindén, M (2009). Targeted intracellular delivery of hydrophobic agents using mesoporous hybrid silica nanoparticles as carrier systems. *Nano Lett* **9**: 3308–3311.
42. Phillips, E, Penate-Medina, O, Zanzonico, PB, Carvajal, RD, Mohan, P, Ye, Y *et al.* (2014). Clinical translation of an ultrasmall inorganic optical-PET imaging nanoparticle probe. *Sci Transl Med* **6**: 260ra149.
43. Niemelä, E, Desai, D, Nkizinkiko, Y, Eriksson, JE and Rosenholm, JM (2015). Sugar-decorated mesoporous silica nanoparticles as delivery vehicles for the poorly soluble drug celastrol enables targeted induction of apoptosis in cancer cells. *Eur J Pharm Biopharm* **96**: 11–21.
44. Espinoza, I and Miele, L (2013). Notch inhibitors for cancer treatment. *Pharmacol Ther* **139**: 95–110.
45. Rizzo, P, Osipo, C, Pannuti, A, Golde, T, Osborne, B and Miele, L (2009). Targeting Notch signaling cross-talk with estrogen receptor and ErbB-2 in breast cancer. *Adv Enzyme Regul* **49**: 134–141.
46. Karaman, DS, Desai, D, Senthilkumar, R, Johansson, EM, Råtts, N, Odén, M *et al.* (2012). Shape engineering vs organic modification of inorganic nanoparticles as a tool for enhancing cellular internalization. *Nanoscale Res Lett* **7**: 358.
47. Chen, J, Hessler, JA, Putchakayala, K, Panama, BK, Khan, DP, Hong, S *et al.* (2009). Cationic nanoparticles induce nanoscale disruption in living cell plasma membranes. *J Phys Chem B* **113**: 11179–11185.
48. Chung, TH, Wu, SH, Yao, M, Lu, CW, Lin, YS, Hung, Y *et al.* (2007). The effect of surface charge on the uptake and biological function of mesoporous silica nanoparticles in 3T3-L1 cells and human mesenchymal stem cells. *Biomaterials* **28**: 2959–2966.
49. Lee, IC, Wang, JH, Lee, YT and Young, TH (2007). Development of a useful technique to discriminate anterior cruciate ligament cells and mesenchymal stem cells–the application of cell electrophoresis. *J Biomed Mater Res A* **82**: 230–237.
50. Galluzzi, L, Kepp, O, Vander Heiden, MG and Kroemer, G (2013). Metabolic targets for cancer therapy. *Nat Rev Drug Discov* **12**: 829–846.
51. Vander Heiden, MG (2011). Targeting cancer metabolism: a therapeutic window opens. *Nat Rev Drug Discov* **10**: 671–684.